VEGF-B gene therapy inhibits doxorubicin-induced cardiotoxicity by endothelial protection

Markus Räsänen[a,b], Joni Degerman[a,b], Tuuli A. Nissinen[c], Ilkka Miinalainen[d], Risto Kerkelä[d], Antti Siltanen[e], Janne T. Backman[f], Eero Mervaala[e], Juha J. Hulmi[c,g], Riikka Kivelä[a,b,1,2], and Kari Alitalo[a,b,1,2]

[a]Wihuri Research Institute, Biomedicum Helsinki, Haartmaninkatu 8, 00290 Helsinki, Finland; [b]Translational Cancer Biology Program, Faculty of Medicine, Biomedicum Helsinki, University of Helsinki, 00014 Helsinki, Finland; [c]Department of Biology of Physical Activity, University of Jyväskylä, 40014 Jyvaskyla, Finland; [d]Medical Research Center Oulu, Research Unit of Biomedicine, University of Oulu and University Hospital Oulu, 90014 Oulu, Finland; [e]Department of Pharmacology, Faculty of Medicine, University of Helsinki, 00014 Helsinki, Finland; [f]Department of Clinical Pharmacology, Faculty of Medicine, University of Helsinki and Helsinki University Hospital, 00014 Helsinki, Finland; and [g]Department of Physiology, Faculty of Medicine, University of Helsinki and Helsinki University Hospital, 00014 Helsinki, Finland

Contributed by Kari Alitalo, September 29, 2016 (sent for review May 26, 2016; reviewed by Mauro Giacca, Joseph C. Wu, and Christian Zuppinger)

Congestive heart failure is one of the leading causes of disability in long-term survivors of cancer. The anthracycline antibiotic doxorubicin (DOX) is used to treat a variety of cancers, but its utility is limited by its cumulative cardiotoxicity. As advances in cancer treatment have decreased cancer mortality, DOX-induced cardiomyopathy has become an increasing problem. However, the current means to alleviate the cardiotoxicity of DOX are limited. We considered that vascular endothelial growth factor-B (VEGF-B), which promotes coronary arteriogenesis, physiological cardiac hypertrophy, and ischemia resistance, could be an interesting candidate for prevention of DOX-induced cardiotoxicity and congestive heart failure. To study this, we administered an adeno-associated viral vector expressing VEGF-B or control vector to normal and tumor-bearing mice 1 wk before DOX treatment, using doses mimicking the concentrations used in the clinics. VEGF-B treatment completely inhibited the DOX-induced cardiac atrophy and whole-body wasting. VEGF-B also prevented capillary rarefaction in the heart and improved endothelial function in DOX-treated mice. VEGF-B also protected cultured endothelial cells from apoptosis and restored their tube formation. VEGF-B increased left ventricular volume without compromising cardiac function, reduced the expression of genes associated with pathological remodeling, and improved cardiac mitochondrial respiration. Importantly, VEGF-B did not affect serum or tissue concentrations of DOX or augment tumor growth. By inhibiting DOX-induced endothelial damage, VEGF-B could provide a novel therapeutic possibility for the prevention of chemotherapy-associated cardiotoxicity in cancer patients.

VEGFB | heart | cancer | endothelial cell | heart failure

Cancer mortality has decreased during the last decades; thus, the number of patients suffering from the long-term effects of cardiotoxic antineoplastic drugs is increasing. Several agents used in cancer treatment can adversely affect the heart and lead to congestive heart failure, which is a growing problem in cardio-oncology. Reversible cardiac changes occur, e.g., during monoclonal antibody therapy with trastuzumab, whereas anthracyclines are associated with cumulative dose-limiting toxicity, which can lead to irreversible cardiac changes and ultimately to dilated cardiomyopathy with long-term heart problems (1, 2).

Doxorubicin (DOX) is an anthracycline cytostatic agent, which has been in clinical use for almost a half century. DOX and other anthracyclines arrest the cell cycle and thus inhibit the proliferation of malignant cells (3). DOX is known to be effective against a wide variety of cancers, which is in part why it has remained one of the most commonly used antineoplastic drugs. However, soon after its discovery, cumulative doses of DOX were found to be harmful also to healthy tissues, especially to the myocardium (4). Cumulative DOX doses are associated with cardiotoxicity, which leads to left ventricular dysfunction and development of heart failure. The toxic mechanisms have been suggested to include mitochondrial iron accumulation and associated redox reactions (5), abnormal protein processing, activation of innate immune responses, DNA damage, failure of cardiac repair, and decreased vasculature (6).

Weight loss in cancer cachexia affects skeletal muscle and adipose tissue and also internal organs including the liver, kidneys, lungs, and heart. Both large tumors and anticancer treatments can cause cachexia alone or in combination (7). Generally, the term "cardiac cachexia" refers to the unintentional weight loss caused by heart disease. However, in the case of cancer cachexia, cardiac cachexia describes the cardiac atrophy, remodeling, and dysfunction associated with cancer (7).

Endothelial dysfunction occurs in many diseases, but endothelial cells (ECs) are seldom considered as therapeutic targets, although many cardiac problems arise as a result of vascular defects (8). Vascular endothelial growth factor-B (VEGF-B) is the least studied member of the five known VEGFs that regulate the proliferation, sprouting, and migration of ECs (9). The highest endogenous concentrations of VEGF-B are found in cardiomyocytes (9). Exogenous VEGF-B is a potent arteriogenic growth factor that can promote physiological cardiac hypertrophy and counteract metabolic problems of obesity (10–12). Furthermore, reduced VEGF-B expression occurs in dilated cardiomyopathy and

Significance

The cardiotoxicity of anthracyclines is a major problem in cancer chemotherapy, and its alleviation would improve the life expectancy of cancer patients. This study shows that vascular endothelial growth factor-B (VEGF-B) gene therapy can be used to prevent the cardiotoxicity of doxorubicin (DOX). VEGF-B inhibited DOX-induced cardiac atrophy, protected endothelial cells from apoptosis, and preserved the myocardial capillary network. Importantly, DOX-induced whole body wasting (cachexia), which both impairs the quality of life and increases drug toxicity in patients as well as decreases their survival, was inhibited by VEGF-B treatment in the DOX-treated mice. Additional preclinical studies are needed for development of the VEGF-B gene therapy for cardiac protection in patients.

Author contributions: M.R., J.J.H., R. Kivelä, and K.A. designed research; M.R., J.D., T.A.N., I.M., R. Kerkelä, A.S., and R. Kivelä performed research; J.T.B., E.M., and J.J.H. contributed new reagents/analytic tools; M.R., J.D., T.A.N., I.M., R. Kerkelä, J.T.B., E.M., J.J.H., R. Kivelä, and K.A. analyzed data; and M.R., R. Kivelä, and K.A. wrote the paper.

Reviewers: M.G., International Centre for Genetic Engineering and Biotechnology; J.C.W., Stanford University School of Medicine; and C.Z., Bern University Hospital.

The authors declare no conflict of interest.

Data deposition: The data reported in this paper have been deposited in the Gene Expression Omnibus (GEO) database, www.ncbi.nlm.nih.gov/geo (accession no. GSE81448).

[1]R. Kivelä and K.A. contributed equally to this work.

[2]To whom correspondence may be addressed. Email: kari.alitalo@helsinki.fi or riikka.kivela@helsinki.fi.

This article contains supporting information online at www.pnas.org/lookup/suppl/doi:10.1073/pnas.1616168113/-/DCSupplemental.

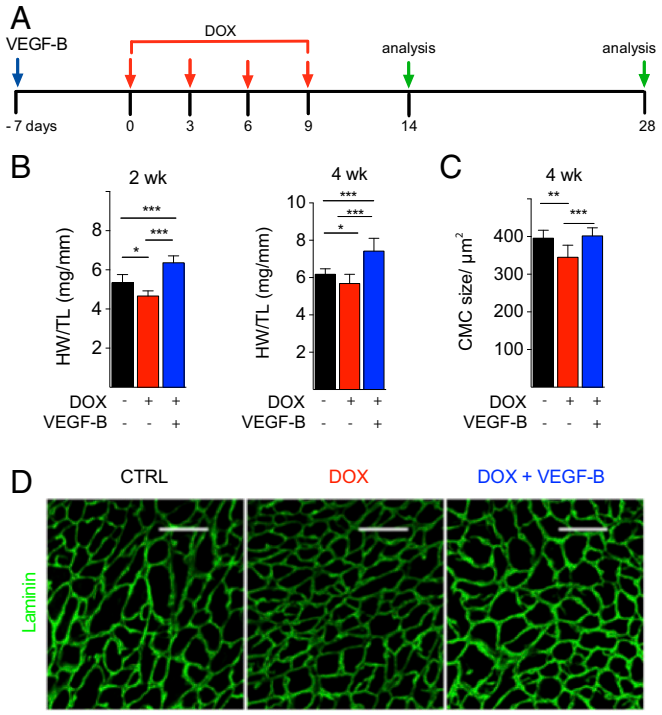

Fig. 1. DOX-induced cardiac atrophy is inhibited by VEGF-B. (*A*) Schedule of the 4- and 2-wk experiments. The mice received four doses of DOX (6 mg/kg) or PBS every 3 d, as indicated. (*B*) Heart weight/tibial length (HW/TL) and (*C*) quantitation of the cardiomyocyte (CMC) size. (*D*) Representative images of laminin staining for cardiomyocyte size analysis. Mean ± SD. $*P = 0.05$; $**P = 0.01$; $***P = 0.001$.

in ischemic heart disease, and VEGF-B has been suggested as a candidate for the therapy of dilated cardiomyopathy (11, 13–16). Interestingly, exogenous VEGF-B maintained mitochondrial respiratory complex 1 function after ischemia/reperfusion injury and protected the heart from ischemic damage (11).

In this study, we have addressed the protective effects of VEGF-B in anthracycline-treated mice. We treated normal and tumor-bearing mice with DOX, which induced damage to the cardiac microvasculature and cardiomyocyte atrophy. We show that these adverse effects, as well as the DOX-induced decrease in lean body mass, can be prevented by VEGF-B gene therapy. Importantly, VEGF-B treatment did not affect the therapeutic levels of DOX or augment tumor growth.

Results

DOX-Induced Cardiac Atrophy Is Inhibited by VEGF-B. To analyze the effects of VEGF-B in DOX-treated mice, we injected adeno-associated viral vector 9 (AAV9)–control vector or AAV9–VEGF-B186 i.p. to the mice 7 d before the first DOX injection (6 mg/kg). DOX treatment was repeated every third day for four times, and the mice were terminated at 2 or 4 wk (Fig. 1*A*). VEGF-B transgene expression in the heart was confirmed by quantitative polymerase chain reaction (qPCR) and ELISA, and VEGF-B serum levels were measured by ELISA (Fig. S1). We also analyzed VEGF-B expression in other tissues after AAV delivery and found the highest levels in the liver, heart, and epididymal adipose tissue (Fig. S2). This is in line with our previously published findings on VEGF-B levels in different tissues after systemic AAV9 delivery (12).

DOX treatment induced significant cardiac atrophy after the cumulative 24 mg/kg dose (Fig. 1*B*). Importantly, the reduction in heart weight and cardiomyocyte size was completely inhibited by pretreatment with AAV–VEGF-B (Fig. 1 *B*–*D*). In addition, left ventricle (LV) posterior wall and septum thickness were decreased after DOX treatment in hearts fixed in diastole, and this was prevented by VEGF-B pretreatment (Fig. S3*C*). DOX treatment also resulted in whole-body cachexia, mainly due to reduced fat and muscle mass (Fig. 2). AAV–VEGF-B inhibited the loss of body mass both in the 2- and 4-wk experiments, but it did not affect body weight in normal untreated mice (Fig. 2 and Fig. S4). VEGF-B did not affect food consumption, which was decreased by 12% in the DOX group and by 10% in the DOX + AAV–VEGF-B group during DOX treatment. Dual-energy X-ray absometry (DXA) analysis of body composition showed similar loss of fat mass in both DOX and DOX + VEGF-B groups, but the lean body mass was significantly higher in the VEGF-B–treated group (Fig. 2 *E*–*G*). However, VEGF-B did not rescue the decrease in bone mineral density (BMD) or maximal running capacity of the DOX-treated mice (Fig. S5).

VEGF-B Protects Cardiac ECs from DOX-Induced Damage. DOX cardiotoxicity has been attributed mainly to cardiomyocyte damage, but because VEGF-B acts via binding to its receptor vascular endothelial growth factor receptor-1 (VEGFR-1), which is expressed in ECs at robustly higher levels than in cardiomyocytes (17), we analyzed the effects of DOX on cardiac microvasculature. DOX caused EC damage in coronary microvasculature and reduced cardiac capillary area significantly in both 2- and 4-wk experiments (Figs. 3*A* and 4). Importantly, this reduction was completely prevented by VEGF-B-treatment (Fig. 3*A*).

To further assess if VEGF-B protects cardiac endothelium from DOX-induced apoptosis, we studied human cardiac microvascular and arterial ECs (HCMECs and HCAECs) in culture. The cells were incubated with conditioned medium from either AAV–VEGF-B or AAV–human serum albumin (HSA) transduced 293T cells, after which the ECs were exposed to DOX. Video microscopy using fluorescent Caspase3/7 activity reporter showed that DOX induced EC apoptosis, which was alleviated by VEGF-B (Fig. 3*B*).

Electron microscopic images of the DOX-treated hearts showed damaged endothelium and mitochondria as well as significant myofibrillar degradation (Fig. 4). The number of cardiomyocytes with disturbed myofibrillar and sarcolemmal integrity tended to

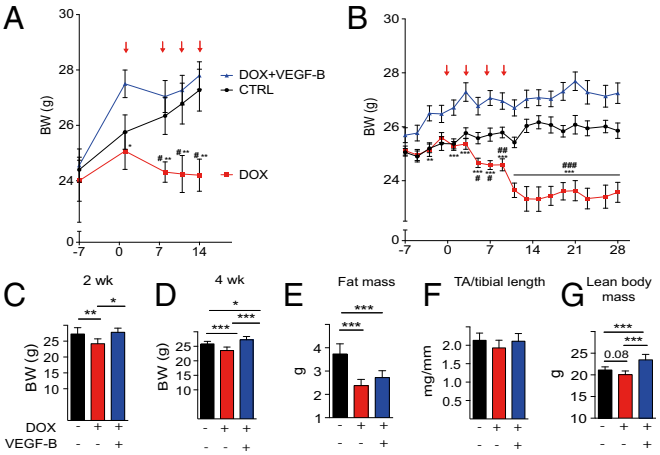

Fig. 2. DOX-induced whole-body wasting is inhibited by VEGF-B. (*A*) Body weight follow-up during the 2-wk experiment and (*B*) 4-wk experiment. (*C* and *D*) Body weights at the end of the experiments. (*E*) Fat mass analyzed by DXA at 4 wk. (*F*) Tibialis anterior muscle weight adjusted to tibial length at 4 wk. (*G*) Lean body mass analyzed by DXA at 4 wk. Arrows indicate the time points of DOX or PBS injections (VEGF-B injections were performed 7 d before the first DOX treatment). Mean ± SD. $*P = 0.05$; $**P = 0.01$; $***P = 0.001$ (DOX vs. DOX + VEGF-B). $^{\#}P = 0.05$; $^{\#\#}P = 0.01$; $^{\#\#\#}P = 0.001$ (DOX vs. CTRL).

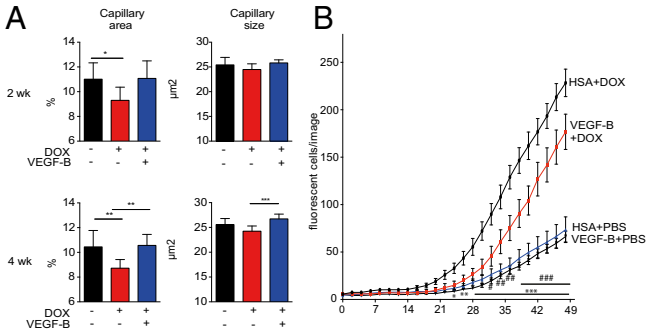

Fig. 3. VEGF-B protects the endothelium against DOX-induced apoptosis and capillary rarefaction. (*A*) Quantification of cardiac capillary area and in DOX and DOX + VEGF-B–treated mice in the 2- and 4-wk experiments compared with the control mice. (*B*) Human arterial ECs were pretreated with medium from AAV9–VEGF-B or AAV9–HSA-transfected 293T cells, followed by administration of DOX (0.5 µM). Apoptosis (Caspase3/7 activity) was analyzed for 48 h by fluorescent time-lapse imaging. $^{*}P = 0.05$; $^{**}P = 0.01$; $^{***}P = 0.001$ (DOX vs. DOX + VEGF-B). $^{\#}P = 0.05$; $^{\#\#}P = 0.01$; $^{\#\#\#}P = 0.001$ (DOX vs. CTRL). Mean ± SD.

decrease in the hearts of mice treated with VEGF-B (30.5 ± 11.4 vs. 19.3 ± 13.2 cells per mm^2, $P = 0.2$) (Mann–Whitney *U* test).

VEGF-B pretreatment also inhibited endothelial dysfunction induced by DOX in the assay of aortic relaxation to acetylcholine (ACh) after phenylephrine-induced contraction. Fig. 5*A* shows significantly improved aortic relaxation in the VEGF-B–pretreated mice in comparison with the DOX-treated mice (Fig. 5*A*). Inhibition of the endothelium-dependent vascular relaxation by $N^{[omega]}$-nitro-L-arginine methyl ester (L-NAME) abolished the differences (Fig. S6). We also observed significant up-regulation of heat shock protein 70 in the DOX-treated but not in DOX + VEGF-B–treated ECs (Fig. S7*A*). As another measure of endothelial dysfunction, HCAEC tube formation on Geltrex matrix was significantly inhibited by 0.5 µmol/L DOX, but this was restored by VEGF-B treatment (Fig. 5 *B* and *C*).

VEGF-B Restores pERK1/2 Signaling in DOX-Treated Hearts. ERK signaling is an important mediator of angiogenesis and arteriogenesis downstream of VEGFR2 activation, and VEGF-B increases ERK1/2 phosphorylation in the heart (10, 18). Here were found that DOX treatment significantly reduced ERK1/2 phosphorylation, which was reversed by VEGF-B (Fig. 6*A*). Consistent with its effect on heart weight, VEGF-B also increased phosphorylation of the ribosomal protein pS6, which is one of the main regulators of the mTOR pathway necessary for cardiomyocyte growth (19) (Fig. 6*B*).

VEGF-B Decreases DOX-Induced DNA Damage and Induction of Markers of Pathological Cardiac Remodeling. To analyze the acute cardiac effects of DOX treatment, we injected 15 mg/kg of DOX intraperitoneally and collected the hearts 20 h after the injection. Cardiac sections were stained for phosphorylated histone H2Ax (γH2Ax), which is used as a marker for the cellular response to DNA double-strand breaks (20). DOX increased the amount of γH2Ax-positive cells significantly compared with PBS, and this effect was attenuated by VEGF-B pretreatment (Fig. 7 *A* and *B*). Terminal deoxynucleotidyl transferase dUTP nick end labeling (TUNEL) showed a trend toward increased DNA fragmentation after DOX treatment in both cardiomyocytes and ECs, but this was not statistically significant (Fig. S7*B*).

Microarray analysis revealed that acute DOX treatment up-regulated the expression of 46 known transcripts and down-regulated 25 known transcripts in the heart [false discovery rate (FDR) < 0.05]. VEGF-B together with DOX in turn up-regulated 1,111 and down-regulated 927 known transcripts. According to the Venn diagram, expression of 16 genes (8 up and 8 down) was significantly changed only in the DOX-treated hearts but not in the VEGF-B + DOX-treated hearts (Fig. S8). Interestingly, the DNA damage-inducible transcript 4 (Ddit4/REDD1), which mediates cardiomyocyte autophagy and apoptosis through the mTOR pathway (21), was one of the significantly increased transcripts in DOX- but not in VEGF-B + DOX-treated hearts (Fig. 7*C*). Furthermore, DOX significantly increased the expression of BNP, ANP, and β-MHC, which are markers of pathological cardiac remodeling, and this was significantly inhibited by VEGF-B (Fig. 7 *D*–*F*). GSEA pathway analysis indicated increased apoptotic signaling and decreased voltage-gated channel activity and cardiac contraction in DOX-treated hearts (Fig. S8). VEGF-B treatment increased cytoskeleton biogenesis, angiogenesis, and cell cycle-related transcripts compared with both control and DOX-treated hearts (Fig. S8).

Effect of VEGF-B on Cardiac and Mitochondrial Function in the DOX-Treated Mice. To assess the effect of DOX and VEGF-B on cardiac function, we carried out echocardiographic analyses after DOX treatment. Ventricular ejection fraction or fractional shortening was not significantly altered in mice treated with DOX for 2 or 4 wk. VEGF-B + DOX treatment increased LV mass and systolic and diastolic LV volumes (Fig. S3) but did not have any adverse effects on cardiac function.

Intact vasculature is necessary for optimal mitochondrial function, as blood vessels provide nutrients and oxygen for cardiomyocyte mitochondria. To analyze the effect of DOX treatment on cardiac mitochondrial function, we performed high-resolution oxygraph analysis of myocardial samples from the LV 3 d after the last DOX injection.

VEGF-B increased mitochondrial oxygen consumption in the DOX-treated hearts when complex I substrates (malate, pyruvate, and glutamate) were used in ADP-stimulated state 3 respiration analysis (Fig. S9*A*). In addition, maximal uncoupled respiration (ETS) was significantly enhanced. To test if this is due to differences in the number of mitochondria, we analyzed cardiac mitochondrial DNA (mtDNA) content. There was a significant increase in total mtDNA in the DOX + VEGF-B group compared with DOX and control groups (Fig. S9*B*). However, there was no difference in expression of peroxisome proliferator-activated receptor gamma co-activator 1 (PGC-1α), which is a major regulator of mitochondrial biosynthesis (Fig. S9*B*).

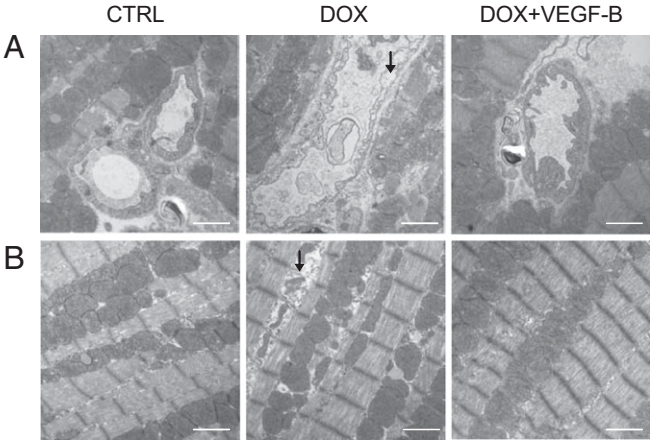

Fig. 4. DOX-induced endothelial and cardiomyocyte damage. Electron microscopic images from hearts of mice treated with PBS (Ctrl), DOX, and VEGF-B + DOX. (*A*) Arrow points to damaged EC in the mouse treated with DOX. (*B*) Arrow points to damaged and atrophied mitochondria in mice treated with DOX. (Scale bar, 2 µm.)

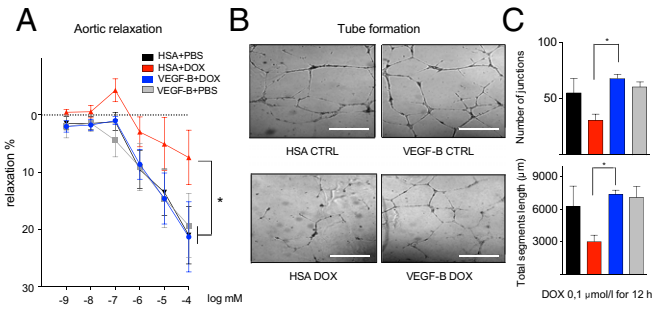

Fig. 5. VEGF-B protects against DOX-induced endothelial dysfunction both in vivo and in vitro. (*A*) Aortic relaxation after phenylephrine contraction and descending ACh concentrations in mice after DOX treatment. (*B*) HCAEC 3D tube formation in Geltrex-coated wells. Cells were pretreated with VEGF-B or HSA as a control and then exposed to DOX (0.5 μM). (*C*) Quantification of the number of junctions and total segment length. Mean ± SD. $*P = 0.05$.

VEGF-B Does Not Affect Tumor Growth or Tissue Concentrations of DOX. To mimic the use of DOX in the clinic, we implanted Lewis lung carcinoma (LLC) cells s.c. to isogenic C57Bl6 mice. AAV–VEGF-B or AAV–Control was administered on day 3 after tumor implantation, and DOX was injected on days 6 and 11. These data indicated that VEGF-B administration did not affect the growth of the LLC xenotransplants (Fig. 8 *B* and *C*). DOX treatment induced significant cardiac and whole-body atrophy in the tumor-bearing mice, which was inhibited by VEGF-B (Fig. 8 *D*–*F*).

To assess if VEGF-B affects DOX availability in target tissues, we measured DOX concentrations in serum, heart, and tumor tissue. These measurements did not reveal significant differences in DOX concentrations between the DOX- and DOX + VEGF-B–treated groups (Fig. 8*G*). Thus, the protective effects of VEGF-B were not due to reduced availability of DOX.

Discussion

Here we show that VEGF-B treatment, starting 1 wk before DOX administration, completely inhibits DOX-induced cardiac atrophy and whole-body wasting, demonstrating a promising anticachexia effect. VEGF-B also prevented capillary rarefaction and protected ECs from apoptosis, improved endothelial and mitochondrial function, and reduced DNA damage. Importantly, VEGF-B treatment did not affect tumor growth or the availability or efficacy of DOX.

Cancer cachexia-related cardiac problems begin with an early atrophy of the LV, which is followed by thinning of the septal and interventricular walls and chamber dilation (7). In later stages, systolic and diastolic dysfunction become evident, accompanied by increased fibrosis and, in the most severe cases, heart failure (7). The decreased LV mass, left ventricular wall and septum thickness, diastolic and systolic volume, and stroke volume in the DOX-treated hearts were prevented by VEGF-B pretreatment. Previous echocardiographic studies have reported a DOX-induced decrease in fractional shortening and ventricular ejection fraction (5, 6). However, our DOX dosing protocol at 24 mg/kg (equivalent to ~72 mg/m^2 in humans) was designed to mimic patient treatment with low DOX doses (30–90 mg/m^2) (22). This dosing did not cause functional systolic impairment during the 2- and 4-wk follow-up. Importantly, there were no deaths in any of the DOX-treated groups in any of the experiments. In human patients, decreased ejection fraction is usually not seen until advanced heart failure, when it is a predictor of a poor prognosis.

Whole-body wasting is shown to be an independent risk factor for mortality in chronic heart failure (23), and it increases chemotherapy toxicity and decreases survival (24). Importantly, although VEGF-B inhibited DOX-induced whole-body wasting in all experiments, it did not increase body weight in healthy mice without cachexia, as we have reported previously (10, 11). Mechanistically, VEGF-B increased phosphorylation of ERK1/2, a downstream mediator of VEGF receptor signaling in the heart, and ribosomal protein S6, indicating activation of the mTORC1 pathway. The effect of VEGF-B is consistent with our previous studies, in which VEGF-B induced mild cardiac and cardiomyocyte hypertrophy that was not converted to cardiomyopathy even upon prolonged VEGF-B overexpression (10, 11). This may be because VEGF-B–induced cardiomyocyte hypertrophy is based on enhanced signaling by endogenous VEGF via endothelial VEGFR2, leading to a concomitant increase of the coronary vasculature (11).

Several mechanisms have been suggested to mediate DOX-induced toxicity to cardiomyocytes (4, 25), whereas endothelial injury has received little attention (26, 27). In our experiments, the apoptosis-associated DNA fragmentation was observed approximately to the same extent in cardiomyocytes and ECs. DOX-induced apoptosis of ECs and capillary rarefaction in mouse hearts was inhibited by VEGF-B. Furthermore, VEGF-B had a protective effect against DOX-induced endothelial dysfunction both in vivo and in vitro, which supports our hypothesis that besides its direct toxicity to cardiomyocytes, DOX induces cardiac damage via ECs by disturbing the protective endothelial–cardiomyocyte cross-talk.

DOX-induced DNA damage in cardiomyocytes, estimated by staining for phosphorylated γH2Ax, a marker of DNA double-strand breakpoints (20), was significantly inhibited by VEGF-B. Furthermore, DOX induction of another DNA damage marker, Ddit4 mRNA, was inhibited by VEGF-B. The gene expression pathway analysis indicated increased apoptosis signaling and decreased expression of genes involved in cardiac contraction in the DOX-treated hearts. Interestingly, the DOX-induced changes in the cardiac transcriptome were similar to those recently reported in human induced pluripotent stem cell-derived cardiomyocytes treated with DOX (28). Previous studies have shown that VEGF-B can protect cultured rat neonatal cardiomyocytes against reactive oxygen species or chemotherapy-induced damage

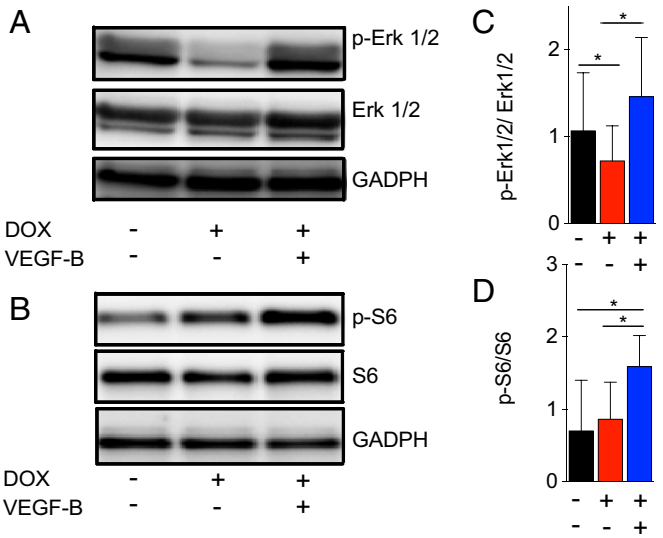

Fig. 6. VEGF-B restores DOX-induced reduction in ERK1/2 phosphorylation and increases phosphorylation of S6. (*A*) Western blot of p-Erk1/2 and total Erk1/2; GADPH was used as a loading control. (*B*) Western blot of p-S6 and total S6. (*C*) Quantification of p-Erk1/2/total Erk1/2 and (*D*) p-S6/total S6. Mean ± SD. $*P = 0.05$. (Scale bar, 50 μm.)

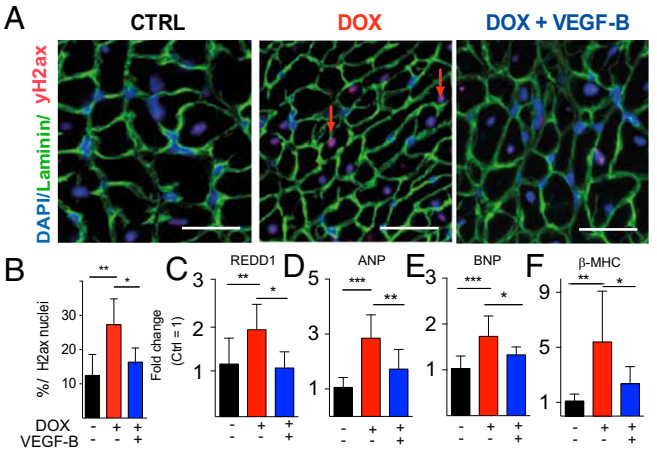

Fig. 7. VEGF-B attenuates DOX-induced DNA damage in cardiomyocytes and inhibits the up-regulation of pathological cardiac transcripts. (*A*) Representative images of immunofluorescence stainings for γH2Ax (red), laminin (green), and DAPI (blue) in cardiac sections. (*B*) Quantification of the percentage of γH2Ax-positive nuclei. mRNA expression of (*C*) REDD1, (*D*) ANP, (*E*) BNP, and (*F*) β-MHC. All values are presented as a fold change compared with the control group. Mean ± SD. $*P = 0.05$; $**P = 0.01$; $***P = 0.001$. (Scale bar, 300 μm.)

(16, 17). Even though the majority of VEGFR1 in the heart is found in ECs (11), VEGF-B may thus protect both ECs and cardiomyocytes against anthracyclin-induced damage.

In agreement with previous reports (29), DOX treatment tended to decrease cardiac mitochondrial complex I activity, whereas VEGF-B treatment increased the activity. This is consistent with our previous data showing that VEGF-B protects against ischemia reperfusion-induced mitochondrial dysfunction (11). The generation of reactive oxygen species (ROS) in cardiomyocytes is known to cause myocardial damage during cancer therapy, especially when anthracyclines are used (30). Sildenafil is cardioprotective against DOX-induced myocardial injury, presumably because it activates the nitric oxide pathway, which opens up the mitochondrial ATP-sensitive potassium channels (31). We have shown that VEGF-B up-regulates endogenous VEGF–VEGFR2 signaling and endothelial nitric oxide synthase (eNOS) expression, which is likely to increase NO production by ECs (11). This is consistent with our present finding that VEGF-B protected against DOX-induced endothelial dysfunction and endothelial tube formation.

Considering the translational potential of the present findings, it was important to confirm that VEGF-B does not compromise therapeutic DOX levels or promote tumor growth. In a previous study, overexpression of VEGF-B was actually shown to inhibit tumor growth, and tumors in VEGF-B–deficient mice grew faster (32). However, we did not experiment with enforced overexpression of VEGF-B in transfected tumor cells, which has been claimed to increase metastasis of tumor grafts via a VEGFR1-independent mechanism (33). Our results, and the fact that unlike other VEGF family members VEGF-B does not promote significantly increased vascular permeability or inflammation, thus encourage further studies on the translational potential of VEGF-B.

Cardiotoxicity limits the successful use of several cytotoxic anticancer agents. Thus, prevention of cardiac atrophy and dysfunction could improve the efficacy of cancer chemotherapy and enhance the chances of patient survival. Our present study demonstrates cardioprotective effects of VEGF-B gene therapy in an anthracycline-induced cardiotoxicity model in mice. VEGF-B inhibited the loss of body and heart weight and protected against DOX-induced DNA damage and mitochondrial dysfunction but did not induce tumor growth. Thus, VEGF-B could provide a safe and effective clinical treatment to alleviate cardiac problems related to cancer treatment, which is in line with previous studies showing beneficial effects of VEGFB in different models of cardiac disease (11, 16, 34). Importantly, our results highlight the possibility of protecting the heart via the vascular endothelium and suggest that VEGF-B could be useful in the therapy of those cardiac disorders where cardiac endothelium plays a pathogenic role.

Methods

A detailed description of the materials and methods can be found in *SI Methods*.

Study Design. In the 2-wk ($n = 6$ per group) and 4-wk ($n = 7$ per group) experiments to mimic chronic DOX exposure, the mice in the DOX and DOX + VEGF-B groups were injected i.p. with 6 mg/kg of DOX every 3 d, four times total; the control mice received PBS (5). To mimic the acute toxicity, we injected 15 mg/kg DOX hydrochloride (Sigma-Aldrich), diluted in 2.5 mL of PBS solution, 20 h before the mice ($n = 7$ per group) were killed. In all experiments, AAV9–mVEGF-B_{186} (2×10^{11} AAV particles) was administered 7 d before the first DOX

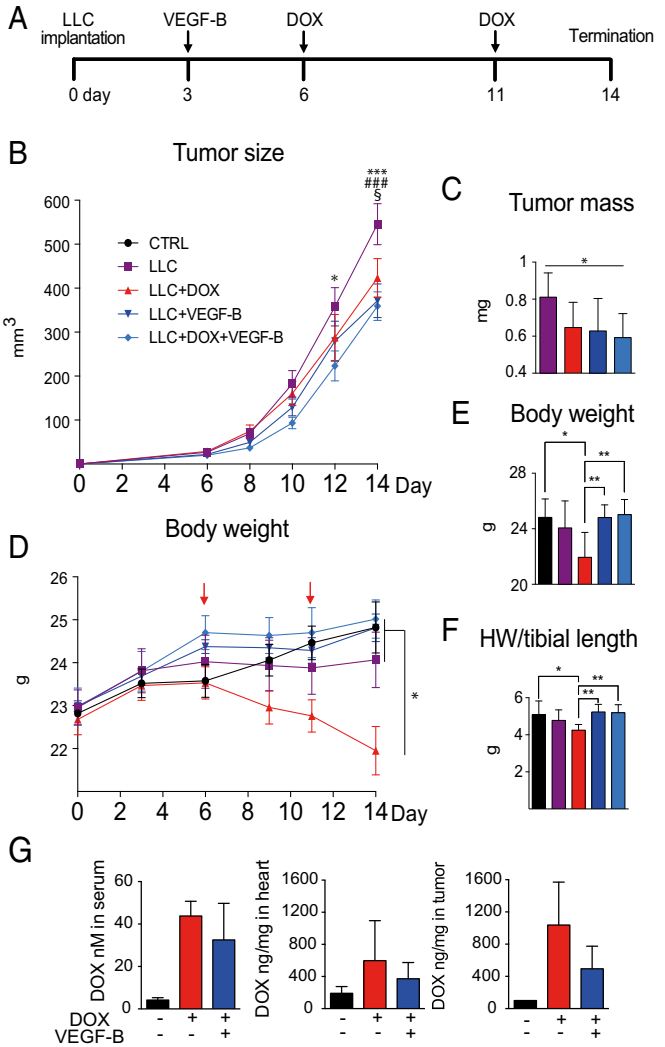

Fig. 8. VEGF-B restores body weight and cardiac mass in DOX-treated LLC tumor-bearing mice but does not increase tumor growth. (*A*) Schedule of the experiment. (*B*) Tumor growth curves and (*C*) tumor tissue mass at termination. (*D*) Body weight follow-up and (*E*) body weight and (*F*) heart weight adjusted to tibial length at termination. (*G*) DOX concentrations in vivo in serum, heart, and tumor tissue. $*P = 0.05$; $**P = 0.01$; $***P = 0.001$ (LLC + DOX vs. LLC + DOX + VEGF-B). $^{\#\#\#}P = 0.001$(LLC + DOX vs. LLC + VEGF-B). $^{\S}P = 0.05$ (LLC vs. LLC+DOX). Mean ± SD.

injection. The control mice were injected with the same amount of scrambled control vector (AAV9-Ctrl) at the same time.

In the 2-wk tumor experiment, the mice were injected s.c. with 5×10^5 LLC cells at day 0. AAV9–mVEGF-B_{186} or control vector was injected i.p. on day 3. The mice received injections of 6 mg/kg DOX on days 6 and 11. All mouse experiments were approved by the Provincial State Office of Southern Finland and carried out in accordance with institutional guidelines. Detailed study design is described in *SI Methods*.

RT-qPCR and Western Blot Analysis. RT-qPCR and Western blot analysis are detailed in *SI Methods*. Primers used are listed in Table S1.

Immunohistochemical Analyses. Frozen sections 8 μm were fixed with acetone, immunostained, and analyzed as detailed in *SI Methods*.

Whole-Genome Microarray and Data Analysis. RNA samples were analyzed with genome-wide Illumina MouseWG-6 v2 microarrays (Illumina Inc.). Detailed microarray data analysis is described in *SI Methods*. The microarray data have been submitted to the GEO database, under the series accession number GSE81448.

Statistical Analysis. Values are indicated as mean ± SD. Statistical analysis of multiple groups was performed with one-way or two-way ANOVAs, followed by Bonferroni or Holm–Sidak post hoc tests. All statistical tests were two-tailed. Differences were considered statistically significant at $P \leq 0.05$. In graphs, $*P \leq 0.05$, $**P \leq 0.01$, and $***P \leq 0.001$.

ACKNOWLEDGMENTS. We thank Dr. Ulrich Pohl, Dr. Andrey Anisimov, and Dr. Su Ngyuen for their helpful comments and Robert Leigh for proofreading the manuscript. Karthik Amudhala Hemanthakumar, Tanja Laakkonen, Maria Arrano-Kivikko, Kirsi Lintula, Tapio Tainola, Maija Atuegwu, Jennifer Paech, and Jouko Laitila are acknowledged for excellent technical assistance. We also thank the Biomedicum Imaging Unit, the AAV Gene Transfer and Cell Therapy Core Facility of Biocenter Finland, as well as the Laboratory Animal Centre of the University of Helsinki for professional services. Funding was provided by the Wihuri Foundation, Academy of Finland (including TCB-CoE Grants 271845 and 275922), Cancer Society of Finland, Sigrid Juselius Foundation, European Research Council (Grant ERC-2010-AdG-268804), and the Leducq Foundation (Grant 11CVD03). M.R. received support from the People Programme (Marie Curie Actions) of the European Union's Seventh Framework Programme FP7/2007-2013 under REA Grant 317250 and M.R. and R. Kivelä from the Finnish Foundation for Cardiovascular Research.

1. Suter TM, Ewer MS (2013) Cancer drugs and the heart: Importance and management. *Eur Heart J* 34(15):1102–1111.
2. Yu AF, Steingart RM, Fuster V (2014) Cardiomyopathy associated with cancer therapy. *J Card Fail* 20(11):841–852.
3. Tacar O, Sriamornsak P, Dass CR (2013) Doxorubicin: An update on anticancer molecular action, toxicity and novel drug delivery systems. *J Pharm Pharmacol* 65(2): 157–170.
4. Nitiss KC, Nitiss JL (2014) Twisting and Ironing: Doxorubicin cardiotoxicity by mitochondrial DNA damage. *Clin Cancer Res* 20(18):4737–4739.
5. Ichikawa Y, et al. (2014) Cardiotoxicity of doxorubicin is mediated through mitochondrial iron accumulation. *J Clin Invest* 124(2):617–630.
6. Zhang S, et al. (2012) Identification of the molecular basis of doxorubicin-induced cardiotoxicity. *Nat Med* 18(11):1639–1642.
7. Murphy KT (2016) The pathogenesis and treatment of cardiac atrophy in cancer cachexia. *Am J Physiol Heart Circ Physiol* 310(4):H466–H477.
8. Heusch G, et al. (2014) Cardiovascular remodelling in coronary artery disease and heart failure. *Lancet* 383(9932):1933–1943.
9. Bry M, Kivelä R, Leppänen VM, Alitalo K (2014) Vascular endothelial growth factor-B in physiology and disease. *Physiol Rev* 94(3):779–794.
10. Bry M, et al. (2010) Vascular endothelial growth factor-B acts as a coronary growth factor in transgenic rats without inducing angiogenesis, vascular leak, or inflammation. *Circulation* 122(17):1725–1733.
11. Kivelä R, et al. (2014) VEGF-B-induced vascular growth leads to metabolic reprogramming and ischemia resistance in the heart. *EMBO Mol Med* 6(3):307–321.
12. Robciuc MR, et al. (2016) VEGFB/VEGFR1-induced expansion of adipose vasculature counteracts obesity and related metabolic complications. *Cell Metab* 23(4):712–724.
13. Huusko J, et al. (2010) The effects of VEGF-R1 and VEGF-R2 ligands on angiogenic responses and left ventricular function in mice. *Cardiovasc Res* 86(1):122–130.
14. Devaux Y, Azuaje F, Vausort M, Yvorra C, Wagner DR (2010) Integrated protein network and microarray analysis to identify potential biomarkers after myocardial infarction. *Funct Integr Genomics* 10(3):329–337.
15. Devaux Y, et al. (2012) Low levels of vascular endothelial growth factor B predict left ventricular remodeling after acute myocardial infarction. *J Card Fail* 18(4):330–337.
16. Woitek F, et al. (2015) Intracoronary cytoprotective gene therapy: A study of VEGF-B167 in a pre-clinical animal model of dilated cardiomyopathy. *J Am Coll Cardiol* 66(2):139–153.
17. Zentilin L, et al. (2010) Cardiomyocyte VEGFR-1 activation by VEGF-B induces compensatory hypertrophy and preserves cardiac function after myocardial infarction. *FASEB J* 24(5):1467–1478.
18. Simons M, Eichmann A (2015) Molecular controls of arterial morphogenesis. *Circ Res* 116(10):1712–1724.
19. Chong ZZ, Shang YC, Maiese K (2011) Cardiovascular disease and mTOR signaling. *Trends Cardiovasc Med* 21(5):151–155.
20. Siddiqui MS, François M, Fenech MF, Leifert WR (2015) Persistent γH2AX: A promising molecular marker of DNA damage and aging. *Mutat Res Rev Mutat Res* 766:1–19.
21. Chen R, et al. (2016) DNA damage-inducible transcript 4 (DDIT4) mediates methamphetamine-induced autophagy and apoptosis through mTOR signaling pathway in cardiomyocytes. *Toxicol Appl Pharmacol* 295:1–11.
22. Vejpongsa P, Yeh ET (2014) Prevention of anthracycline-induced cardiotoxicity: Challenges and opportunities. *J Am Coll Cardiol* 64(9):938–945.
23. Anker SD, et al. (1997) Wasting as independent risk factor for mortality in chronic heart failure. *Lancet* 349(9058):1050–1053.
24. Kazemi-Bajestani SM, Mazurak VC, Baracos V (2016) Computed tomography-defined muscle and fat wasting are associated with cancer clinical outcomes. *Semin Cell Dev Biol* 54:2–10.
25. Madonna R, et al. (2015) Improving the preclinical models for the study of chemotherapy-induced cardiotoxicity: A position paper of the Italian Working Group on Drug Cardiotoxicity and Cardioprotection. *Heart Fail Rev* 20(5):621–631.
26. Yin Z, et al. (2016) miR-320a mediates doxorubicin-induced cardiotoxicity by targeting VEGF signal pathway. *Aging (Albany, NY)* 8(1):192–207.
27. Sun Z, et al. (2016) The TGF-β pathway mediates doxorubicin effects on cardiac endothelial cells. *J Mol Cell Cardiol* 90:129–138.
28. Burridge PW, et al. (2016) Human induced pluripotent stem cell-derived cardiomyocytes recapitulate the predilection of breast cancer patients to doxorubicin-induced cardiotoxicity. *Nat Med* 22(5):547–556.
29. Marques-Aleixo I, et al. (2015) Physical exercise prior and during treatment reduces sub-chronic doxorubicin-induced mitochondrial toxicity and oxidative stress. *Mitochondrion* 20:22–33.
30. Belmonte F, et al. (2015) ErbB2 overexpression upregulates antioxidant enzymes, reduces basal levels of reactive oxygen species, and protects against doxorubicin cardiotoxicity. *Am J Physiol Heart Circ Physiol* 309(8):H1271–H1280.
31. Das A, Durrant D, Salloum FN, Xi L, Kukreja RC (2015) PDE5 inhibitors as therapeutics for heart disease, diabetes and cancer. *Pharmacol Ther* 147:12–21.
32. Albrecht I, et al. (2010) Suppressive effects of vascular endothelial growth factor-B on tumor growth in a mouse model of pancreatic neuroendocrine tumorigenesis. *PLoS One* 5(11):e14109.
33. Yang X, et al. (2015) VEGF-B promotes cancer metastasis through a VEGF-A-independent mechanism and serves as a marker of poor prognosis for cancer patients. *Proc Natl Acad Sci USA* 112(22):E2900–E2909.
34. Pepe M, et al. (2010) Intramyocardial VEGF-B167 gene delivery delays the progression towards congestive failure in dogs with pacing-induced dilated cardiomyopathy. *Circ Res* 106(12):1893–1903.
35. Pesta D, Gnaiger E (2012) High-resolution respirometry: OXPHOS protocols for human cells and permeabilized fibers from small biopsies of human muscle. *Methods Mol Biol* 810:25–58.
36. Kallio MA, et al. (2011) Chipster: User-friendly analysis software for microarray and other high-throughput data. *BMC Genomics* 12:507.
37. Mootha VK, et al. (2003) PGC-1alpha-responsive genes involved in oxidative phosphorylation are coordinately downregulated in human diabetes. *Nat Genet* 34(3): 267–273.
38. Subramanian A, et al. (2005) Gene set enrichment analysis: A knowledge-based approach for interpreting genome-wide expression profiles. *Proc Natl Acad Sci USA* 102(43):15545–15550.
39. Ma W, Wang J, Guo Q, Tu P (2015) Simultaneous determination of doxorubicin and curcumin in rat plasma by LC-MS/MS and its application to pharmacokinetic study. *J Pharm Biomed Anal* 111:215–221.